J. Fluid Mech. (2003), *vol.* 477, *pp.* 321–337. © 2003 Cambridge University Press
DOI: 10.1017/S0022112002003282 Printed in the United Kingdom

Quasi-static solutions for quantum vortex motion under the localized induction approximation

By TOMASZ LIPNIACKI

Institute of Fundamental Technological Research, Świętokrzyska St. 21, 00-049 Warsaw, Poland
tlipnia@ippt.gov.pl

(Received 21 March 2002 and in revised form 6 August 2002)

The motion of a quantum vortex is considered in the context of the localized induction approximation (LIA). In this context, the instantaneous vortex velocity is proportional to the local curvature and is parallel to the vector which is a linear combination of the local binormal and the principal normal to the vortex line. This implies that the quantum vortex shrinks, which is in contrast to the classical vortex in an ideal fluid. The present work deals with a four-parameter class of static solutions of the equations governing the curvature and the torsion. Such solutions describe vortex lines, the motion of which is equivalent to an isometric transformation. In a particular case when the transformation is a pure translation, the analytic solutions for the curvature and the torsion are found. In the general case, when the transformation is a superposition of a non-trivial translation and rotation, the asymptotics of solutions is explicitly related to the parameters characterizing the transformation, and then to the initial conditions at the zero point of the vortex. In this case, the equations are solved numerically and the shape of a number of different vortices is reconstructed by numerical integration of Frenet–Seret equations.

1. Introduction

According to Landau's two-fluid theory, He II (superfluid ^{4}He) is a sum of the Bose condensate (superfluid component) and the gas of thermal excitation (normal component). The rotationless flow of the superfluid component is violated on one-dimensional singularities, called quantum vortices. There is a variety of the dynamic phenomena exhibited by superfluid ^{4}He involving the appearance and motion of quantized vortices (see Nemirowskii & Fiszdon 1995 for a comprehensive review). Because of these singularities, the superfluid component is coupled dissipatively with the normal component.

The circulation of the superfluid velocity about these lines remains constant, $\kappa = h/m_{He} = 9.97 \times 10^{-4}$ cm^2 s^{-1}, where h is Planck's constant, and m_{He} is the mass of a helium atom. The curve traced out by a vortex filament may be specified in the parametric form $\boldsymbol{s}(\xi, t)$, with t and ξ denoting time and arclength, respectively.

The self-induced velocity at a given point of a vortex $\boldsymbol{s}(\xi, t)$ is described by the Biot-Savart integral

$$\boldsymbol{V}_i(\boldsymbol{s}(\xi, t)) = \frac{\kappa}{4\pi} \int \frac{(\boldsymbol{s}(\xi, t) - \boldsymbol{s}(\bar{\xi}, t)) \times \boldsymbol{s}'(\bar{\xi}, t)}{|\boldsymbol{s}(\xi, t) - \boldsymbol{s}(\bar{\xi}, t)|^3} \, \mathrm{d}\bar{\xi}, \tag{1.1}$$

where the prime denotes an instantaneous derivative with respect to ξ, and the integral is taken over all vortex lines excluding the neighbourhood of point $\boldsymbol{s}(\xi, t)$ (of

https://doi.org/10.1017/S0022112002003282 Published online by Cambridge University Press

radius equal to the effective vortex core radius $a_o \approx 1.3 \times 10^{-8}$ Å). The approach to vortex dynamics via the Biot-Savart law usually leads to time-consuming numerical simulations, but may offer a deeper insight into coupled dynamics of the two helium components (Barenghi *et al.* 1997; Idowu *et al.* 2000). Here, we follow the approach of Schwarz (1985), who concluded that in some cases the Biot-Savart integral can be approximated in terms of the so-called localized induction approximation (LIA), which retains only the effects of the local vortex curvature,

$$\boldsymbol{V}_i = \beta \boldsymbol{s}' \times \boldsymbol{s}'', \tag{1.2}$$

with

$$\beta = \frac{\kappa}{4\pi} \ln\left(\frac{d}{a_o \langle |\boldsymbol{s}''| \rangle}\right), \tag{1.3}$$

where d is a constant of order one, and $\langle |\boldsymbol{s}''| \rangle$ is the characteristic average curvature of the vortex. Although β has the logarithmic dependence on $\langle |\boldsymbol{s}''| \rangle$, it is usually treated as a constant. The main advantage of LIA is that it describes the vortex motion in a much simpler way than the Biot-Savart law, thus enabling numerical simulations (Schwarz 1988; Schwarz & Rozen 1991) and modelling (Lipniacki 2001*a*, *b*) of the dynamics of the complicated systems of quantum vortices, such as a quantum tangle, which may have kilometres of quantum vortices in 1 cm^3. The approximation seems justified when the local curvature is large enough, so the term $\beta \boldsymbol{s}' \times \boldsymbol{s}''$ is greater than the velocity induced by other vortices, or original vortex segments. Nevertheless, it is very difficult to judge whether a particular vortex configuration can be computed using the localized induction approximation, rather than the full Biot-Savart law, without carrying out both calculations and comparing the results (see Ricca, Samuels & Barenghi 1999). The present work is restricted to LIA.

The influence of the normal fluid leads to the difference between the effective quantum vortex velocity $\dot{\boldsymbol{s}}(\xi, t)$ and $\boldsymbol{V}_i$. The overdot denotes the instantaneous time. The normal fluid exerts the drag force $\boldsymbol{f}_D$ on the vortex.

$$\boldsymbol{f}_D = \bar{\alpha} \rho_s \kappa \boldsymbol{s}' \times [\boldsymbol{s}' \times (\boldsymbol{V}_n - \boldsymbol{V}_s - \boldsymbol{V}_i)] - \alpha' \rho_s \kappa [\boldsymbol{s}' \times (\boldsymbol{V}_n - \boldsymbol{V}_s - \boldsymbol{V}_i)], \tag{1.4}$$

where $\boldsymbol{V}_n$ and $\boldsymbol{V}_s$ are the average superfluid and normal fluid velocities and $\bar{\alpha}$ and α' are temperature-dependent friction coefficients (in the literature $\bar{\alpha}$ is usually denoted by α). The drag force integrated over all vortex lines in a volume gives the mutual friction force, which dissipatively couples the two helium components. This force is balanced by the Magnus force $\boldsymbol{f}_M$, which is exerted on the vortex by the superfluid component and which arises when a body with circulation around it (such as a vortex line) moves in a flow,

$$\boldsymbol{f}_M = \rho_s \kappa \boldsymbol{s}' \times (\dot{\boldsymbol{s}} - \boldsymbol{V}_i - \boldsymbol{V}_s). \tag{1.5}$$

Since the inertia of the vortex core is negligible, the sum of the forces on each line element must vanish,

$$\boldsymbol{f}_M + \boldsymbol{f}_D = 0, \tag{1.6}$$

hence, the resulting instantaneous velocity of a given point of the filament in the localized induction approximation is

$$\dot{\boldsymbol{s}} = \beta \boldsymbol{s}' \times \boldsymbol{s}'' + \boldsymbol{V}_s + \bar{\alpha} \boldsymbol{s}' \times (\boldsymbol{V}_{ns} - \beta \boldsymbol{s}' \times \boldsymbol{s}'') - \alpha' \boldsymbol{s}' \times [\boldsymbol{s}' \times (\boldsymbol{V}_{ns} - \beta \boldsymbol{s}' \times \boldsymbol{s}'')], \tag{1.7}$$

https://doi.org/10.1017/S0022112002003282 Published online by Cambridge University Press

where $\boldsymbol{V}_{ns} = \boldsymbol{V}_n - \boldsymbol{V}_s$. Then, in the absence of both normal and superfluid velocity fields, $\boldsymbol{V}_n = \boldsymbol{V}_s = 0$, (1.7) simplifies to

$$\dot{\boldsymbol{s}} = \beta(1-\alpha')\boldsymbol{s}' \times \boldsymbol{s}'' + \alpha \boldsymbol{s}'' = \beta \boldsymbol{s}' \times \boldsymbol{s}'' + \alpha \boldsymbol{s}'' = c(\beta \boldsymbol{b} + \alpha \boldsymbol{n}), \tag{1.8}$$

where $\alpha = \beta\bar{\alpha}$, c is the local vortex curvature and $\boldsymbol{t}, \boldsymbol{n}$ and $\boldsymbol{b} = \boldsymbol{t} \times \boldsymbol{n}$ are the right-handed system of mutually perpendicular unit vectors parallel to the tangent, principal normal and binormal, respectively. The coefficient α' for temperatures of less than 2.1 K$^\circ$ is much smaller than unity and is usually neglected, or, as in our case ($\boldsymbol{V}_{ns} = 0$), it may be absorbed into the modified β. The main friction coefficient $\bar{\alpha} = \alpha/\beta$, grows from the value of 0.01 up to 1, as temperature grows from 1.07 K$^\circ$ up to 2.15 K$^\circ$, which is close to the λ transition point at 2.17 K$^\circ$. Assuming that both normal and superfluid velocity fields are zero, we assume that the normal fluid component exerts a friction force on the vortex line, but remains unaffected by the motion of the vortex line itself.

The present paper is focused on quasi-static solutions to (1.8) in the infinite three-dimensional domain. Reconnections are not considered. The difference between the motion of a quantum vortex and the classical one (in an ideal fluid) is in the last term of (1.8). For $\alpha = 0$, (1.8) can be transformed to a nonlinear Schrödinger equation (NLSE) for $\Psi = c\exp(\mathrm{i}\int_0^\xi \tau \,\mathrm{d}\bar{\xi})$, where τ is the torsion (see Hasimoto 1972). This helped to show that there are soliton-like solutions describing a loop or a hump propagating along the vortex line. The equivalence to NLSE (for $\alpha = 0$) implies also that the vortex motion is conservative, and there exists a countable family of conserved integral quantities (see Ricca 1992), such as the total length $l = \int \mathrm{d}\xi$, the total torsion $\int \tau \,\mathrm{d}\xi$, the total curvature squared $\int c^2 \,\mathrm{d}\xi$, etc.

As we have said, in superfluid ^{4}He, $\alpha > 0$; this makes the vortex line shrink, and its motion is no longer conservative. Nevertheless, as will be shown, there exists a four-parametric class of solutions to (1.8) for which the vortex line conserves its shape and its spatial scale.

Nakayama, Segur & Wadati (1992) and Onuki (1985) analysed the following equation

$$\dot{\boldsymbol{s}} = U\boldsymbol{n} + V\boldsymbol{b} + W\boldsymbol{t}, \tag{1.9}$$

where U, V and W are functions of curvature, torsion and their derivatives. These authors in their analysis mostly confined themselves to the case $\partial W/\partial s = cU$, which implies that the length of the line is conserved. However, the superfluid vortices, in our approximation, (1.8), move in the direction perpendicular to the local tangent, which implies that there is no tangent stretching ($W = 0$); as a result, the vortex lines shrink, which significantly influences their dynamics. The motion along the normal to the line is also characteristic for thin magnetic tubes, which shrink to minimize their magnetic energy.

The vector equation (1.8) can be transformed into a system of two scalar equations (see Langer & Perline 1991 or Nakayama *et al.* 1992) for the filament curvature $c(\xi, t)$ and torsion $\tau(\xi, t)$:

$$\dot{c} = -\beta(2c'\tau + c\tau') + \alpha(c'' - c\tau^2 + c^3), \tag{1.10}$$

$$\dot{\tau} = \beta\left(\frac{c'' - c\tau^2}{c} + \tfrac{1}{2}c^2\right)' + \alpha\left[\left(\frac{2c'\tau + c\tau'}{c}\right)' + 2\tau c^2\right]. \tag{1.11}$$

For $\alpha = 0$, the above system simplifies to the Da Rios–Betchov equations (see Ricca 1996 for the review), which can be extended to the higher-dimensional case (Ricca

https://doi.org/10.1017/S0022112002003282 Published online by Cambridge University Press

1991). From now on, we will assume that $\alpha > 0$. As we have said, β is proportional to the elementary circulation, what implies $\beta/\alpha > 0$; nevertheless, the case $\beta/\alpha = 0$ will also be considered as a simple instructive example. For $\alpha > 0$, the vortex line shrinks according to the law (Schwarz 1988),

$$\dot{\xi} = \int_0^{\xi} \boldsymbol{s}' \cdot (\dot{\boldsymbol{s}})' \, \mathrm{d}\bar{\xi} = \int_0^{\xi} \boldsymbol{s}' \cdot (\beta(\boldsymbol{s}' \times \boldsymbol{s}'')' + \alpha \boldsymbol{s}''') \, \mathrm{d}\bar{\xi}, \tag{1.12}$$

$$\dot{\xi} = -\alpha \int_0^{\xi} \boldsymbol{s}'' \cdot \boldsymbol{s}'' \, \mathrm{d}\bar{\xi} = -\alpha \int_0^{\xi} c^2 \, \mathrm{d}\bar{\xi}. \tag{1.13}$$

As a result, the partial derivatives of curvature and torsion $\partial c/\partial t$, $\partial \tau/\partial t$ differ from instantaneous derivatives $\dot{c}$, $\dot{\tau}$:

$$\dot{c} = \frac{\partial c}{\partial t} - \alpha c' \int_0^{\xi} c^2 \, \mathrm{d}\bar{\xi}, \tag{1.14}$$

$$\dot{\tau} = \frac{\partial \tau}{\partial t} - \alpha \tau' \int_0^{\xi} c^2 \, \mathrm{d}\bar{\xi}. \tag{1.15}$$

This yields

$$\frac{\partial c}{\partial t} = -\beta(2c'\tau + c\tau') + \alpha(c'' - c\tau^2 + c^3) + \alpha c' \int_0^{\xi} c^2 \, \mathrm{d}\bar{\xi}, \tag{1.16}$$

$$\frac{\partial \tau}{\partial t} = \beta\left(\frac{c'' - c\tau^2}{c} + \frac{c^2}{2}\right)' + \alpha\left[\left(\frac{2c'\tau + c\tau'}{c}\right)' + 2\tau c^2\right] + \alpha\tau' \int_0^{\xi} c^2 \, \mathrm{d}\bar{\xi}. \tag{1.17}$$

Having the curvature and the torsion, we can reconstruct the vortex curve $\boldsymbol{s}(\xi, t)$ with the help of Frenet–Seret equations for the unit tangent $\boldsymbol{t}$, the unit normal $\boldsymbol{n}$ and the unit binormal $\boldsymbol{b} = \boldsymbol{t} \times \boldsymbol{n}$:

$$\boldsymbol{t}' = c\boldsymbol{n}, \quad \boldsymbol{n}' = -c\boldsymbol{t} + \tau\boldsymbol{b}, \quad \boldsymbol{b}' = -\tau\boldsymbol{n}. \tag{1.18a–c}$$

This reconstruction corresponds to the solution of the Riccati equation, whose coefficients are functions of curvature and torsion, and it is a non-trivial task, which can be done only numerically. In this paper, we focus on the quasi-static solutions (i.e. the solutions for which $\partial c/\partial t = \partial \tau/\partial t = 0$) of system (1.16), (1.17).

2. Fundamental equations

For $\partial c/\partial t = \partial \tau/\partial t = 0$, equations (1.16) and (1.17) simplify to a system of ordinary integro-differential equations (OIDEs):

$$0 = -\beta(2c'\tau + c\tau') + \alpha(c'' - c\tau^2 + c^3) + \alpha c' \int_0^{\xi} c^2 \, \mathrm{d}\bar{\xi}, \tag{2.1}$$

$$0 = \beta\left(\frac{c'' - c\tau^2}{c} + \tfrac{1}{2}c^2\right)' + \alpha\left[\left(\frac{2c'\tau + c\tau'}{c}\right)' + 2\tau c^2\right] + \alpha\tau' \int_0^{\xi} c^2 \, \mathrm{d}\bar{\xi}. \tag{2.2}$$

We call the solutions of the above system quasi-static because the fact that the time partial derivatives of the curvature and the torsion vanish, does not imply that the vortex line does not move. It moves and shrinks and an observer sitting on a given point of the vortex may see that both the local curvature and the local torsion change

https://doi.org/10.1017/S0022112002003282 Published online by Cambridge University Press

($\dot{c} \neq 0, \dot{\tau} \neq 0$), but still as a curve the vortex remains unchanged in the sense that there exists an isometric transformation $\mathscr{T}(t)$ transforming $\boldsymbol{s}(\xi, 0)$ onto $\boldsymbol{s}(\xi, t)$ for any $t \in R$. This paradox comes from the fact that the vortex shrinks and the position ξ of the observer sitting on a vortex changes (equation (1.13)). Moreover, as we will see, all the quasi-static solutions correspond to vortices of infinite length, which means that they may shrink, and still remain unchanged. The isometric transformation $\mathscr{T}(t)$ can be uniquely represented as a superposition ($\mathscr{T} = \mathscr{T}_{\mathscr{T}} \circ \mathscr{T}_{\mathscr{R}}$) of translation $\mathscr{T}_{\mathscr{T}}$ and rotation $\mathscr{T}_{\mathscr{R}}$ around an axis parallel to the translation vector. This can be used to derive (2.1) and (2.2) in an alternative way, but also to find a particular class of analytic solutions to this system. Moreover, the analysis of the transformation enables us to connect by means of an analytic expression asymptotics of a given solution with the 'initial conditions' $c_0 = c(0)$, $c_0' = c'(0)$, $\tau_0 = \tau(0)$, $\tau_0' = \tau'(0)$.

Let $\boldsymbol{W}(t)$ be the translation vector and $\Omega(t)$ the rotation operator, then we have

$$\boldsymbol{s}(\xi, t) = \boldsymbol{W}(t) + \Omega(t)\boldsymbol{s}(\xi, 0). \tag{2.3}$$

Differentiating (2.3) in t we obtain

$$c(\beta \boldsymbol{b} + \alpha \boldsymbol{n}) + \alpha \boldsymbol{t} \int_0^{\xi} c^2 \, \mathrm{d}\bar{\xi} = \boldsymbol{V} + \boldsymbol{\omega} \times \boldsymbol{s}(\xi, 0), \tag{2.4}$$

where $\boldsymbol{V} = \mathrm{d}\boldsymbol{W}/\mathrm{d}t$ is the linear velocity of the vortex, while $\boldsymbol{\omega}$, the angular velocity, satisfies $\boldsymbol{\omega} \times \boldsymbol{s}(\xi, 0) = (\mathrm{d}/\mathrm{d}t)(\Omega(t)\boldsymbol{s}(\xi, 0))$. Note, that since, in general, $\dot{\boldsymbol{s}} \neq \boldsymbol{V} + \boldsymbol{\omega} \times \boldsymbol{s}(\xi, 0)$, the observer sitting on a filament moves with velocity different from $\boldsymbol{V} + \boldsymbol{\omega} \times \boldsymbol{s}(\xi, 0)$. Differentiating (2.4) with respect to ξ and using Frenet–Seret formulae, (1.18), we have

$$c'(\beta \boldsymbol{b} + \alpha \boldsymbol{n}) + c\tau(-\beta \boldsymbol{n} + \alpha \boldsymbol{b}) + \alpha c \boldsymbol{n} \int_0^{\xi} c^2 \, \mathrm{d}\bar{\xi} = \boldsymbol{\omega} \times \boldsymbol{t}. \tag{2.5}$$

Since $\boldsymbol{t} = \boldsymbol{n} \times \boldsymbol{b}$, we have $\boldsymbol{\omega} \times \boldsymbol{t} = \boldsymbol{n}(\boldsymbol{b} \cdot \boldsymbol{\omega}) - \boldsymbol{b}(\boldsymbol{n} \cdot \boldsymbol{\omega})$. Now, multiplying (2.5) in turn by $\boldsymbol{b}$ and by $\boldsymbol{n}$, we obtain, respectively,

$$\beta c' + \alpha c\tau = -\boldsymbol{n} \cdot \boldsymbol{\omega}, \tag{2.6}$$

and

$$\alpha c' - \beta c\tau + \alpha c \int_0^{\xi} c^2 \, \mathrm{d}\bar{\xi} = \boldsymbol{b} \cdot \boldsymbol{\omega}. \tag{2.7}$$

Differentiating (2.6) and (2.7) with respect to ξ, we have

$$\beta c'' + \alpha(c\tau)' = (c\boldsymbol{t} - \tau \boldsymbol{b}) \cdot \boldsymbol{\omega}, \tag{2.8}$$

and

$$\alpha c'' - \beta(c\tau)' + \alpha \left(c \int_0^{\xi} c^2 \, \mathrm{d}\bar{\xi} \right)' = -\tau \boldsymbol{n} \cdot \boldsymbol{\omega}. \tag{2.9}$$

Substituting $\boldsymbol{n} \cdot \boldsymbol{\omega}$ from (2.6) into (2.9), we obtain

$$\alpha c'' - \beta(c\tau)' + \alpha \left(c \int_0^{\xi} c^2 \, \mathrm{d}\bar{\xi} \right)' = \tau(\beta c' + \alpha c\tau), \tag{2.10}$$

which is equivalent to (2.1). Then substituting $\boldsymbol{b} \cdot \boldsymbol{\omega}$ from (2.7) into (2.8) we have:

$$\beta c'' + \alpha(c\tau)' + \tau \left(\alpha c' - \beta c\tau + \alpha c \int_0^{\xi} c^2 \, \mathrm{d}\bar{\xi} \right) = c\boldsymbol{t} \cdot \boldsymbol{\omega}. \tag{2.11}$$

https://doi.org/10.1017/S0022112002003282 Published online by Cambridge University Press

Now, dividing both sides of (2.11) by c, differentiating and using equality $\boldsymbol{t}'\cdot\boldsymbol{\omega} = -c(\beta c' + \alpha c\tau)$, which follows from the first Frenet–Seret relation (1.18a) and (2.6), we obtain

$$\left(\frac{\beta c'' + \alpha(c\tau)' + \tau\left(\alpha c' - \beta c\tau + \alpha c\int_0^\xi c^2\,\mathrm{d}\bar{\xi}\right)}{c}\right)' = -c(\beta c' + \alpha c\tau), \tag{2.12}$$

which is equivalent to (2.2). This completes the alternative derivation of (2.1) and (2.2).

Now, we relate the parameters characterizing transformation $\mathscr{T}$, to the initial conditions $c_0 = c(0), c_0' = c'(0), \tau_0 = \tau(0), \tau_0' = \tau'(0)$ of the corresponding solution. From (2.4), it follows that the point $\xi = 0$ of the filament moves along a helix (or in the particular case along a line or a circle),

$$\dot{\boldsymbol{s}}(0) = c(\beta\boldsymbol{b} + \alpha\boldsymbol{n}) = \boldsymbol{V} + \boldsymbol{\omega}\times\boldsymbol{s}(0). \tag{2.13}$$

If $\omega = 0$, then

$$V = c_0\sqrt{\beta^2+\alpha^2}. \tag{2.14}$$

If $\boldsymbol{\omega} \neq 0$, then let $R_0 = |\boldsymbol{\omega}\times\boldsymbol{s}(0)|/\omega$ denote the helix radius or the distance between the point $\xi = 0$ and the axis of rotation, and let γ be the angle between $\dot{\boldsymbol{s}}(0)$ and $\boldsymbol{\omega}$. Note that, since $\dot{\boldsymbol{s}}(0)$ has no radial component, the pair R_0, γ characterizes the vortex position with respect to the axis of rotation. From (2.13) we have

$$V = \cos(\gamma)c_0\sqrt{\beta^2+\alpha^2}, \tag{2.15}$$

$$\omega R_0 = \sin(\gamma)c_0\sqrt{\beta^2+\alpha^2}. \tag{2.16}$$

Now, multiplying (2.6) by α and (2.7) by $-\beta$ and adding the results together, we have (for $\xi = 0$)

$$(\beta^2+\alpha^2)c_0\tau_0 = -(\alpha\boldsymbol{n} + \beta\boldsymbol{b})\cdot\boldsymbol{\omega}, \tag{2.17}$$

$$\cos(\gamma) = -\frac{c_0\tau_0\sqrt{\beta^2+\alpha^2}}{\omega}. \tag{2.18}$$

From (2.10), we calculate c'' and substitute it into (2.11) to obtain

$$-\beta c_0^2 + \frac{\beta^2+\alpha^2}{\alpha}\left(\frac{2c_0'\tau_0 + c_0\tau_0'}{c_0}\right) = \boldsymbol{t}\cdot\boldsymbol{\omega}. \tag{2.19}$$

Since $\omega^2 = (\boldsymbol{t}\cdot\boldsymbol{\omega})^2 + |\boldsymbol{t}\times\boldsymbol{\omega}|^2$ it follows from (2.5) and (2.19), that

$$\omega^2 = \left(-\beta c_0^2 + \frac{\beta^2+\alpha^2}{\alpha}\left(\frac{2c_0'\tau_0 + c_0\tau_0'}{c_0}\right)\right)^2 + (\beta^2+\alpha^2)\left((c_0')^2 + c_0^2\tau_0^2\right). \tag{2.20}$$

Equations (2.15), (2.16), (2.18) and (2.20) relate the initial conditions of the solution to the parameters ω, V, R_0 and γ characterizing the corresponding transformation.

In the next two sections, we analyse the two particular cases

(i) $\omega = 0$ and $\mathscr{T} = \mathscr{T}_{\mathscr{T}}$,

(ii) $V = 0$ and $\mathscr{T} = \mathscr{T}_{\mathscr{R}}$.

Restricting, from now on, the analysis to the curves without inflection points which implies in particular that $c_0 > 0$, we may conclude from the above analysis that:

if $\omega = 0$, then it follows from (2.20) that $\tau_0' = c_0^2\alpha\beta/(\alpha^2+\beta^2), c_0' = 0, \tau_0 = 0$;

if $V = 0$, then it follows from (2.15) and (2.18) that $\tau_0 = 0$.

Except for the first case ($\boldsymbol{\omega} = 0$), system (2.1), (2.2) cannot be simplified and will be analysed with the help of numeric calculations. To enable numerical analysis of

https://doi.org/10.1017/S0022112002003282 Published online by Cambridge University Press

the system we transform it into the form in which $c'' = c''(c, c', \tau, \tau')$, and $\tau'' = \tau''(c, c', c'', \tau, \tau')$. From (2.1), we obtain:

$$c'' = (c\tau^2 - c^3) + \frac{\beta}{\alpha}(2c'\tau + c\tau') - c'\int_0^\xi c^2 \,\mathrm{d}\bar{\xi}. \tag{2.21}$$

To obtain the expression for τ'', we can calculate c''' by differentiating (2.21) and inserting it into (2.2). From the resulting equation, we extract τ''

$$\tau'' = \frac{1}{\alpha^2+\beta^2}\left[\alpha\beta\left(\frac{c'c''}{c^2} - \frac{c'\tau^2}{c} + 3cc' + \frac{c''}{c}\int_0^\xi c^2 \,\mathrm{d}\bar{\xi}\right)\right.$$
$$\left. + \alpha^2\left(\frac{2c'^2\tau}{c^2} - \frac{2(c''\tau + c'\tau')}{c} - 2\tau c^2 - \tau'\int_0^\xi c^2 \,\mathrm{d}\,\bar{\xi}\right) - \beta^2\left(\frac{2c''\tau + 3c'\tau'}{c}\right)\right]. \tag{2.22}$$

Any solution to system (2.21), (2.22) is determined by a set of four initial conditions c_0, c_0', τ_0 and τ_0'. However, since the system is invariant under the following transformation

$$\xi \hookrightarrow \xi/\lambda, \quad c \hookrightarrow \lambda c, \quad \tau \hookrightarrow \lambda\tau, \tag{2.23}$$

all solutions with initial conditions $\lambda c_0, \lambda^2 c_0', \lambda\tau_0$ and $\lambda^2\tau_0'$ determine one family of similar curves with spatial scale inversely proportional to λ.

The other important transformation which leaves the system invariant is

$$\xi \hookrightarrow -\xi, \quad c \hookrightarrow c, \quad \tau \hookrightarrow -\tau. \tag{2.24}$$

This implies, that there exists a class of symmetric solutions for which $c(\xi) = c(-\xi)$ and $\tau(\xi) = -\tau(-\xi)$. These solutions describe curves having a plane of symmetry perpendicular to the tangent to the curve at $\xi = 0$. Since, for any such solution $c_0' = \tau_0 = 0$, the corresponding transformation is a pure rotation or a pure translation.

3. The case $\mathscr{T} = \mathscr{T}_{\mathscr{F}}$ – the analytic solutions

For $\omega = 0$, (2.6) and (2.7) simplify to

$$\tau = -\frac{\beta c'}{\alpha c}, \tag{3.1}$$

and

$$\left(\frac{\alpha^2+\beta^2}{\alpha^2}\right)c' = -c\int_0^\xi c^2 \,\mathrm{d}\bar{\xi}. \tag{3.2}$$

We multiply (3.2) by $2c$, set $y(\xi) = \int_0^\xi c^2 \,\mathrm{d}\bar{\xi}$ and integrate to obtain

$$\left(\frac{\alpha^2+\beta^2}{\alpha^2}\right)y' = c_0^2 - y^2, \tag{3.3}$$

where $c_0 = c(0)$. After solving (3.3), we obtain $c = \sqrt{y'}$, and then we have τ from (3.1)

$$c = c_0 \operatorname{sech}(A\xi), \quad \tau = B\tanh(Al), \tag{3.4}$$

where

$$A = \frac{\alpha c_0}{\sqrt{\alpha^2+\beta^2}}, \quad B = \frac{\beta c_0}{\sqrt{\alpha^2+\beta^2}}. \tag{3.5}$$

https://doi.org/10.1017/S0022112002003282 Published online by Cambridge University Press

It can be checked now, that the above solution is a particular solution of system (2.21), (2.22); nevertheless, it seems difficult to obtain it directly from (2.21), (2.22). The solution has only one free parameter $c_0 = c(0)$, while $c_0' = \tau_0 = 0$, $\tau_0' = AB$.

The shape of the filament is determined by $c(\xi)$, $\tau(\xi)$ and Frenet–Seret formulae; nevertheless, in our case, it seems difficult to calculate it that way. To obtain $\boldsymbol{s}(\xi)$ we return to (2.14). Since $V = c_0\sqrt{\alpha^2+\beta^2}$, without lost of generality, we can assume that in Cartesian coordinates $\boldsymbol{V} = (0, 0, c_0\sqrt{\alpha^2+\beta^2})$. Now, multiplying (2.4), for $\omega = 0$, by $\boldsymbol{t}$ we obtain $t_z(\xi)$ (the z component of $\boldsymbol{t}$),

$$t_z = \frac{\alpha\int_0^{\xi} c^2\,\mathrm{d}\bar{\xi}}{c_0\sqrt{\alpha^2+\beta^2}} = \tanh(A\xi). \tag{3.6}$$

From definition $|\boldsymbol{t}|^2 = t_x^2 + t_y^2 + t_z^2 = 1$, and from (1.18$a$), we know that $|\boldsymbol{t}'| = t'^2_x + t'^2_y + t'^2_z = c$. Hence, from (3.6) we obtain two equations for t_x and t_y

$$t_x^2 + t_y^2 = \operatorname{sech}^2(A\xi), \tag{3.7}$$

$$t'^2_x + t'^2_y = \operatorname{sech}^4(A\xi)(c^2\cosh^2(A\xi) - A^2). \tag{3.8}$$

Introducing new variables

$$R = \sqrt{t_x^2 + t_y^2} = |t_x + \mathrm{i}t_y|, \quad t_x + \mathrm{i}t_y = Re^{\mathrm{i}\phi}, \tag{3.9}$$

we obtain

$$R' = A\operatorname{sech}^2(A\xi)\sinh(A\xi), \tag{3.10}$$

$$R'^2 + \phi'^2R^2 = \operatorname{sech}^4(A\xi)(c^2\cosh^2(A\xi) - A^2). \tag{3.11}$$

The above system can be easily solved, namely

$$t_x = R\cos(q\xi), \quad t_y = R\sin(q\xi), \quad t_z = \tanh(A\xi), \tag{3.12}$$

with

$$R = \operatorname{sech}(A\xi), \quad q = \sqrt{c_0^2 - A^2}. \tag{3.13}$$

Finally,

$$\boldsymbol{s}(\xi, t) = \left(\int_{\infty}^{\xi} R\cos(q\xi)\,\mathrm{d}\bar{\xi}, \int_{\infty}^{\xi} R\sin(q\xi)\,\mathrm{d}\bar{\xi}, tc_0\sqrt{\alpha^2+\beta^2} + \ln(\cosh(A\xi))/A\right). \tag{3.14}$$

The shape of the filament $\boldsymbol{s}(\xi, t)$ is determined uniquely by (β/α), while parameter c_0 fixes only the spatial scale of the curve. Figure 1 represents the curve $\boldsymbol{s}(\xi, t)$, calculated for $(\beta/\alpha = 2)$, at two different times. Note that the trajectory of an arbitrarily chosen point $\xi = \xi_0 \neq 0$ differs from the trajectory of the observer sitting on the vortex, at first at $\xi = \xi_0$. For $\beta/\alpha = 0$, the torsion is identically zero and the curve is planar. It follows from the symmetry of solution (3.14) that $s_x(\xi) = -s_x(-\xi)$ and $s_y(\xi) = s_y(-\xi)$, $s_z(\xi) = s_z(-\xi)$. This implies that the corresponding filament has no self-crossing if and only if $s_x(\xi) > 0$ for any $\xi > 0$, or equivalently, since $s_x(\xi)$ has the deepest minimum at $q\xi = \frac{3}{2}\pi$, if and only if $s(3\pi/2q) > 0$. The latter depends on

https://doi.org/10.1017/S0022112002003282 Published online by Cambridge University Press

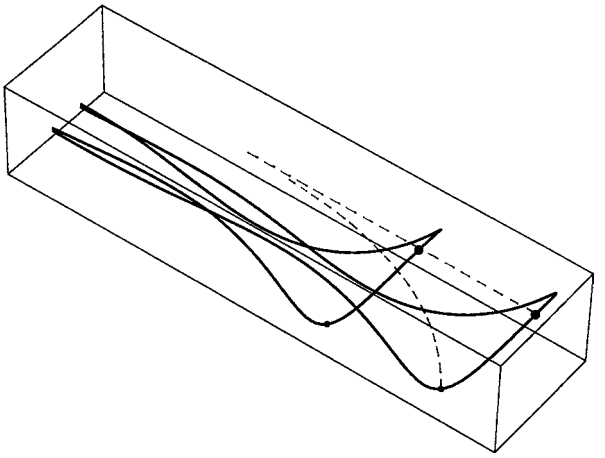


FIGURE 1. The vortex filament $\boldsymbol{s}(\xi, t)$, as described by (3.14) for $\beta/\alpha = 2$, at times t_1 and t_2. The local line motion is equivalent to its pure translation, from right to left. •, $\xi = 0$; ●, $\xi = \xi_0$. – – –, hand-drawn trajectories of the observers being fixed to the vortex, initially at the positions $\xi = 0$ and $\xi = \xi_0$. The observers' trajectories are perpendicular to local instantaneous tangents to the vortex, see (1.8), and, generally, the observer position changes because of the shrinking of the vortex line.

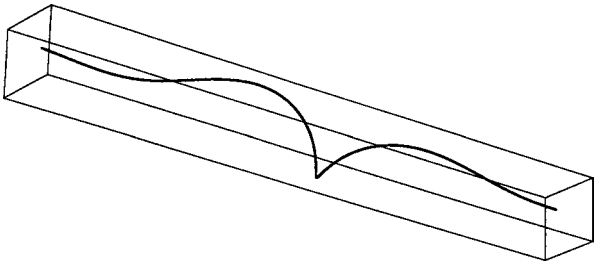


FIGURE 2. The Hasimoto soliton for $c_0 = \tau_0$. For such a choice of parameters, the hump propagates along the line with velocity $2\beta\tau_0$ in the direction of filament vorticity and rotates with angular velocity $\frac{3}{4}\beta\tau_0^2$; the direction of rotation is opposite to the direction of vorticity.

(β/α) and

for $\beta/\alpha < \beta_{cr} : s_x(3\pi/2q) > 0 \Rightarrow$ there are no self-crossings,
for $\beta/\alpha = \beta_{cr} : s_x(3\pi/2q) = 0 \Rightarrow$ filament is self-tangent at $\xi = 3\pi/2q$,
for $\beta/\alpha > \beta_{cr} : s_x(3\pi/2q) < 0 \Rightarrow$ there are two or more self-crossings,

where $\beta_{cr} \approx 2.254$. The number of self-crossings grows with (β/α). Obviously, the solutions with self-crossings have no physical meaning.

At the end off the section we recall the Hasimoto (1972) soliton (see figure 2), for which the curvature $c(\xi, t)$ and the torsion $\tau(\xi, t)$ satisfy:

$$c = c_0 \operatorname{sech}(c_0(\xi - V_0 t)/2), \quad \tau = \tau_0 = \text{const}, \tag{3.15}$$

where $V_0 = 2\beta\tau_0$ is the propagation velocity. The main difference between the Hasimoto solution and ours is that the Hasimoto hump travels along the vortex with velocity V_0, while the centre of our loop also moves in space, but still remains at the point $\xi = 0$ of the vortex. Since the Hasimoto soliton also rotates, with angular

https://doi.org/10.1017/S0022112002003282 Published online by Cambridge University Press

velocity $\omega = \beta[(\frac{1}{4}c_0^2) - \tau_0^2]$, the isometric transformation $\mathscr{T}(t)$, which transforms $\boldsymbol{s}(\xi, 0)$ onto $\boldsymbol{s}(\xi - V_0 t, t)$ is, in general, a superposition of a rotation, around the axis containing the two asymptotes of the vortex, and the translation along that axis. Both the Hasimoto solution and ours, (3.14), describe filaments of infinite length, which evidently may not exist in experimental apparatus. Nevertheless, until our loop or the Hasimoto hump, are far from the vessel boundaries, the solutions are satisfactory approximations of the real dynamics.

4. The case $\mathscr{T} = \mathscr{T}_{\mathscr{R}}$

As we have said, if $\tau_0 = 0, c_0 > 0$, then for arbitrary c_0', τ_0', excluding the case analysed in previous section in which $c_0' = 0, \tau_0' = c_0^2\alpha\beta/(\alpha^2 + \beta^2)$, the corresponding transformation is a pure rotation. In this case, we make use of the hints following from the numerical solutions of system (2.21), (2.22) to derive analytic expressions, which connect the asymptotic behaviour of the solution with initial conditions. The numerical analysis suggests the following asymptotic behaviour of $c(\xi)$ and $\tau(\xi)$:

$$\lim_{\xi\to\pm\infty} c|\xi|^{1/3} = K_0, \quad \lim_{\xi\to\pm\infty} \tau\xi = \mp T_0, \quad T_0 = \frac{\beta}{3\alpha}. \tag{4.1}$$

This result can be justified in the following way. Let us insert $c = K_0/\xi^{1/3}$ and $\tau = -T_0/\xi$ into (2.21), (2.22). The two highest-order terms in (2.21) are then proportional to $1/\xi$, and they cancel for arbitrary K_0 and T_0. In (2.22), the highest-order terms are proportional to $1/\xi^{5/3}$. There are three such terms, and they cancel for $T_0 = \beta/3\alpha$ and arbitrary K_0 (or for $K_0 = 0$). Obviously, this does not prove (4.1), but shows that if $\lim_{\xi\to\pm\infty} c|\xi|^{1/3} = K_0 \neq 0$ and $\lim_{\xi\to\pm\infty} \tau\xi = \mp T_0$, then $T_0 = \beta/3\alpha$.

The required asymptotics, (4.1), of the curvature and the torsion is satisfied by the curve $s(l)$, which in the cylindrical coordinates (r, Θ, z) reads

$$r(l) = \frac{l^{1/3}}{K_0}, \quad \Theta(l) = -\tfrac{3}{2}K_0 l^{2/3}, \quad z(l) = \frac{l^{1/3}\cot(\phi)}{K_0}. \tag{4.2}$$

Parameter l is not the arclength, but since $\lim_{l\to\infty} |\mathrm{d}s/\mathrm{d}l| = 1$, and so $\lim_{l\to\infty} l/\xi = 1$, it can be replaced by the arclength ξ, for ξ sufficiently large. It can be checked by the elementary calculations, that if $\cot(\phi) = \beta/\alpha$, then the curvature and the torsion of $s(l)$ satisfy (4.1). This implies that all the filaments of the considered class must behave asymptotically like the curve $s(l)$, which wraps over a cone with an opening angle 2ϕ. The fragment of the curve for which $\Theta \in (2\pi k, 2\pi(k+1)], k \in N$, will be called a roll. Since Θ changes from $-\infty$ to $+\infty$, the curve consists of the infinite number of rolls. Since $\lim_{\xi\to\pm\infty} t_\Theta = 1$, where t_Θ is the poloidal component of the unit tangent, each roll moves towards the vertex of the cone with the velocity βc and contracts with velocity αc. This implies that it remains on the cone if and only if $\beta/\alpha = \cot(\phi)$, which confirms the numerical prediction (4.1). The motion of the rolls towards the vertex of the cone is equivalent to the uniform rotation of the whole curve. In the limit of infinite $|l|$ or $|\xi|$, the separation $\Delta z(\xi)$ between subsequent rolls (or points of the curve lying on the same generix) calculated along the z-axis, is

$$\Delta z(\xi) = 2\pi r(\xi)\frac{\mathrm{d}z}{\mathrm{d}\xi} = \frac{2\pi\cot(\phi)}{3\xi^{1/3}K_0^2} = \frac{2\pi\beta}{3\alpha\xi^{1/3}K_0^2}. \tag{4.3}$$

https://doi.org/10.1017/S0022112002003282 Published online by Cambridge University Press

Hence, the time P it takes to replace one roll with another is

$$P = \frac{\Delta z(\xi)}{\beta c(\xi)} = \frac{2\pi}{3\alpha K_0^3} = \text{const.} \tag{4.4}$$

Since, the time P does not depend on ξ, we may conclude that the whole curve rotates with angular velocity ω,

$$\omega = 2\pi/P = 3\alpha K_0^3. \tag{4.5}$$

Equations (4.5) and (2.20), for $\tau_0 = 0$, allow us to connect the initial conditions with the asymptotics of the solution:

$$\lim_{\xi\to\pm\infty} c|\xi|^{1/3} = K_0, \quad \lim_{\xi\to\pm\infty} \tau\xi = T_0, \tag{4.6}$$

with

$$K_0 = (3\alpha)^{-1/3}\left[\left(-\beta c_0^2 + \frac{\beta^2+\alpha^2}{\alpha}\tau_0'\right)^2 + (\beta^2+\alpha^2)(c_0')^2\right]^{1/6}, \tag{4.7}$$

$$T_0 = \frac{\beta}{3\alpha}. \tag{4.8}$$

Additionally, we may conclude that all filaments of the considered class wrap asymptotically over two coaxial cones with the same opening angle 2ϕ, $\cot(\phi) = \beta/\alpha$. This conclusion is in a full accordance with the numerical integration of the Frenet–Seret equations for calculated $c(\xi)$ and $\tau(\xi)$, see figure 3.

If, as we have said, $\tau_0 = 0$ and $c_0' = 0$, the resulting curve has a plane of symmetry perpendicular to the axis of rotation. For $c_0' = 0$, (4.7) simplifies to

$$K_0 = (3\alpha)^{-1/3}\left[-\beta c_0^2 + \frac{\beta^2+\alpha^2}{\alpha}\tau_0'\right]^{1/3}. \tag{4.9}$$

Analysing numerically the symmetric case in more detail, we can distinguish two characteristic filament configurations. Let $z = 0$ be the plane of symmetry, then:

$$\left.\begin{aligned} &\lim_{\xi\to\infty} \boldsymbol{t}(0)\boldsymbol{s}(\xi) > 0 \quad \text{for } \tau'(0) \leqslant \tau_{cr}, \\ &\lim_{\xi\to\infty} \boldsymbol{t}(0)\boldsymbol{s}(\xi) < 0 \quad \text{for } \tau'(0) > \tau_{cr}, \end{aligned}\right\} \tag{4.10}$$

where $\tau_{cr} = c^2(0)\alpha\beta/(\alpha^2+\beta^2)$. Recall that, for $\tau'(0) = \tau_{cr}$, the filament has two asymptotes. The solution of the first configuration is presented in figure 3(*a*) and that of the second in figure 3(*b*).

For $\tau'(0) < \tau_{cr}^*$, the filament has no self-crossings, whereas for $\tau'(0) > \tau_{cr}^*$, it has at least one. The value of τ_{cr}^* depends on (β/α), and for $(\beta/\alpha) \leqslant \beta_{cr}$, $\tau_{cr}^* = \tau_{cr}$, whereas for $(\beta/\alpha) > \beta_{cr}$, $\tau_{cr}^* < \tau_{cr}$. For $c_0' \neq 0$, the resulting curves (see figure 3*c*) have no plane of symmetry and, in general, have no self-crossings.

5. The most general case: $\mathscr{T} = \mathscr{T}_{\mathscr{R}} \circ \mathscr{T}_{\mathscr{T}}$

In this section, we discuss the largest class of solutions with initial conditions $\tau_0 \neq 0, c_0 > 0$ and c_0', τ_0' arbitrary. As we have said, in this case, the corresponding transformation $\mathscr{T} = \mathscr{T}_{\mathscr{R}} \circ \mathscr{T}_{\mathscr{T}}$ is a superposition of a non-trivial rotation and a translation.

https://doi.org/10.1017/S0022112002003282 Published online by Cambridge University Press

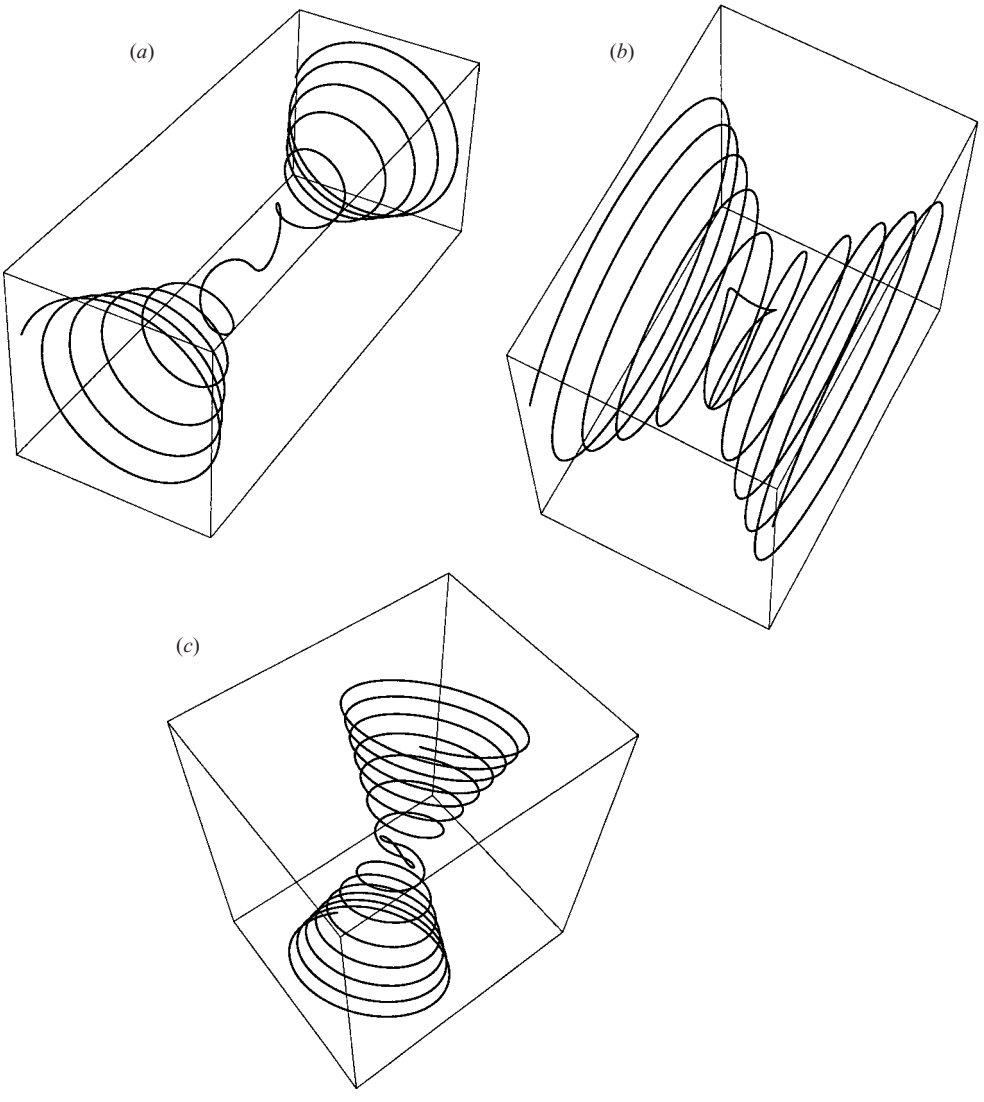


FIGURE 3. The three configurations of vortex filaments, the motion of which is equivalent to pure rotation. The vortex lines wrap asymptotically over two coaxial cones with the same opening angle ϕ, with $\cot(\phi) = \beta/\alpha$. (*a*) The solution with plane of symmetry obtained for $\beta/\alpha = 2$, $\tau_0 = c_0' = 0$, $\tau_0' = -\frac{1}{2}\tau_{cr} = -c_0^2\alpha\beta/2(\alpha^2+\beta^2)$. (*b*) The solution with plane of symmetry obtained for $\beta/\alpha = 1$, $\tau_0 = c_0' = 0$, $\tau_0' = 2\tau_{cr} = 2c_0^2\alpha\beta/(\alpha^2+\beta^2)$. Since the presented curve has a self-crossing, it does not represent any physical filaments. (*c*) The non-symmetric solution obtained for $\beta/\alpha = 2$, $\tau(0) = 0$, $c_0' = c_0^2$, $\tau_0' = \frac{1}{2}c_0^2$.

As in the previous section, we use hints following from numerics to connect the asymptotics of solutions with their initial conditions. The numerical analysis suggests the following asymptotic behaviour of solutions

$$\lim_{\xi\to\pm\infty} c|\xi|^{1/3} = K_0, \quad \lim_{\xi\to\pm\infty} \tau\xi^{2/3} = T_0. \tag{5.1}$$

Let us then insert $c = K_0/\xi^{1/3}$ and $\tau = T_0/\xi^{2/3}$ into (2.21) and (2.22). Then, in (2.21),

https://doi.org/10.1017/S0022112002003282 Published online by Cambridge University Press

the highest-order terms are proportional to $1/\xi$, and they cancel for arbitrary K_0 and T_0. In (2.22), the highest-order terms are now proportional to $1/\xi^{4/3}$, and they also cancel for arbitrary T_0 and K_0.

The required asymptotics, (5.1), of the curvature and the torsion is satisfied by the curve $s(l)$, which in the cylindrical coordinates (r, Θ, z) reads

$$r(l) = \frac{|l|^{1/3}}{K_0}, \quad \Theta(l) = \frac{3K_0 l^{2/3}}{2}, \quad z(l) = \frac{3T_0 l^{2/3}}{K_0}. \tag{5.2}$$

As in the case of $\mathscr{T} = \mathscr{T}_R$, we replace l with ξ. For $|l|$ or $|\xi|$ tending to infinity, the curve $s(l)$ wraps over a paraboloid. Since $s(l)$ has the required asymptotics, we may conclude that the real filaments (see figure 4) also wrap, in the limit of infinite $|\xi|$, over one of two isometric coaxial paraboloids. In the limit of infinite $|\xi|$ (or $|l|$), the separation between subsequent rolls is

$$\Delta z(\xi) = 2\pi r \frac{\mathrm{d}z}{\mathrm{d}\xi} = \frac{2\pi T_0}{K_0^2}. \tag{5.3}$$

The local motion of a vortex is equivalent to its translation with a velocity $\boldsymbol{V}$ superposed with rotation with an angular velocity $\boldsymbol{\omega}$. To calculate the translation velocity we note that since $\lim_{\xi\to\pm\infty} t_\Theta = 1$, where t_Θ is the poloidal component of unit tangent, each roll moves towards the vertex of the paraboloid with velocity βc and contracts with velocity αc. Since βc tends to zero for $|\xi|$ tending to infinity, the self-velocity of rolls is not important for propagation of the whole structure. The motion of the whole filament results from the contraction of the rolls; propagation velocity is

$$V = \frac{\mathrm{d}z}{\mathrm{d}t} = \frac{\mathrm{d}r}{\mathrm{d}t}\frac{\mathrm{d}z}{\mathrm{d}r}. \tag{5.4}$$

Since, from (5.2), $z = \frac{3}{2}K_0 T_0 r^2$, then

$$V = 3\alpha T_0 K_0 = \text{const}. \tag{5.5}$$

The filament rotates with period P, in which every roll is replaced by the next one, $P = h/V = 2\pi/3\alpha K_0^3 = \text{const}$; this gives the rotation velocity ω,

$$\omega = 3\alpha K_0^3 = \text{const}. \tag{5.6}$$

The fact that both V and ω are independent of ξ confirms that the numerically deduced asymptotics of solutions (5.1) is correct. Using (5.5), (5.6) and (2.15), (2.18), (2.20) we can connect the initial conditions with the asymptotics of the solution:

$$\lim_{\xi\to\pm\infty} c|\xi|^{1/3} = K_0, \quad \lim_{\xi\to\pm\infty} \tau\xi^{2/3} = T_0, \tag{5.7}$$

where

$$K_0 = (3\alpha)^{-1/3}\left[\left(-\beta c_0^2 + \frac{\beta^2+\alpha^2}{\alpha}\left(\frac{2c_0'\tau_0 + c_0\tau_0'}{c_0}\right)\right)^2 + (\beta^2+\alpha^2)\big((c_0')^2 + c_0^2\tau_0^2\big)\right]^{1/6}, \tag{5.8}$$

$$T_0 = -\frac{c_0^2\tau_0(\beta^2+\alpha^2)}{9\alpha^2 K_0^4}. \tag{5.9}$$

The fact that the asymptotics of the solutions can be connected to their initial condition, may suggest the existence of some conservation laws for system (2.1), (2.2).

https://doi.org/10.1017/S0022112002003282 Published online by Cambridge University Press

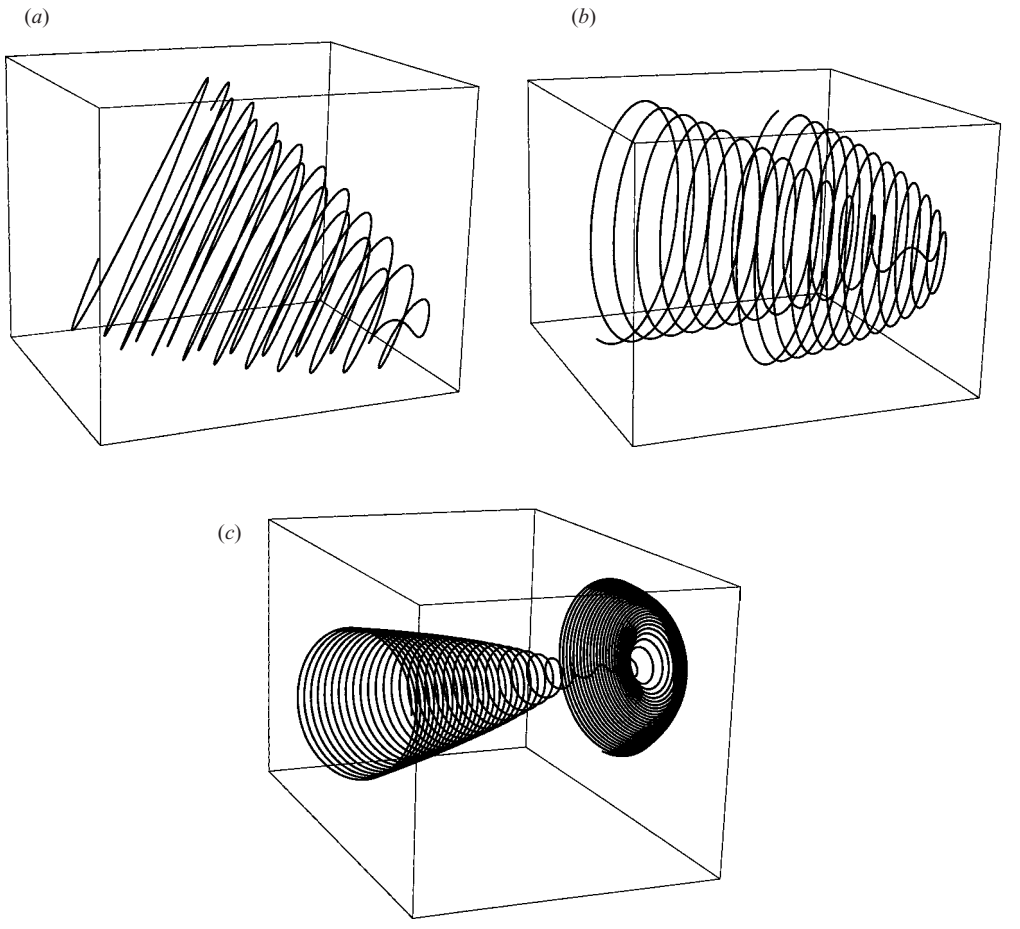


FIGURE 4. The three configurations of vortex filaments, the motion of which is equivalent to the isometric transformation being a superposition of translation and rotation. The vortex lines wrap asymptotically over two coaxial isometric paraboloids. (*a*) The solution obtained for $\beta/\alpha = 0$, $\tau_0 = -\frac{1}{2}c_0$, $c_0' = c_0^2$, $\tau_0' = \frac{1}{2}c_0^2$. (*b*) The solution obtained for $\beta/\alpha = \frac{1}{2}$, $\tau_0 = -\frac{1}{2}c_0$, $c_0' = c_0^2$, $\tau_0' = \frac{1}{2}c_0^2$. (*c*) The solution obtained for $\beta/\alpha = 2$, $\tau_0 = -\frac{1}{2}c_0$, $c_0' = c_0^2$, $\tau_0' = \frac{1}{2}c_0^2$. Asymptotically, the filament wraps over two isometric coaxial paraboloids, but, in this case, the asymptotic behaviour is approached for very large ξ. This is because the filament wraps over each of the paraboloids in opposite directions, and because of relatively large β/α, the local motion of any roll close to the point $\xi = 0$ is significant. For very large $|\xi|$, however, the curvature, and hence the velocity of rolls, becomes negligible. In this limit, both paraboloids move because of the shrinking of the rolls, which is independent of their orientation.

In fact, it is possible to integrate these equations after introducing new variables

$$X = \int_0^{\xi} c^2 \, \mathrm{d}\bar{\xi}, \tag{5.10}$$

$$Y = \int_0^{\xi} \tau c^2 \, \mathrm{d}\bar{\xi}, \tag{5.11}$$

Note that X and Y are conserved quantities in an ideal ($\alpha = 0$) vortex motion. The

https://doi.org/10.1017/S0022112002003282 Published online by Cambridge University Press

resulting equations are complicated, and we have failed to find an analytic solution different from those presented in § 3.

6. Other classes of solution to system (1.16), (1.17)

In this section, we want to draw attention to a class of self-similar solutions to (1.16) and (1.17). Let us note that system (1.16), (1.17) is invariant under the following transformation (Lipniacki 2002)

$$t \hookrightarrow \lambda^2 t, \quad \xi \hookrightarrow \lambda\xi; \text{ the latter implies } c \hookrightarrow \lambda^{-1}c, \quad \tau \hookrightarrow \lambda^{-1}\tau. \tag{6.1}$$

This suggests the introduction of new variables

$$c := \frac{1}{\sqrt{t}}K\left(\frac{\xi}{\sqrt{t}}\right), \quad \tau := \frac{1}{\sqrt{t}}T\left(\frac{\xi}{\sqrt{t}}\right), \quad l := \frac{\xi}{\sqrt{t}}, \tag{6.2}$$

that yield

$$\partial c/\partial t = -\frac{1}{2t^{3/2}}\left(K + l\frac{\partial K}{\partial l}\right), \tag{6.3}$$

$$\partial \tau/\partial t = -\frac{1}{2t^{3/2}}\left(T + l\frac{\partial T}{\partial l}\right), \tag{6.4}$$

$$c' = \frac{1}{t}\frac{\partial K}{\partial l}, \quad c'' = \frac{1}{t^{3/2}}\frac{\partial^2 K}{\partial l^2}, \tag{6.5}$$

$$\tau' = \frac{1}{t}\frac{\partial T}{\partial l}, \quad \tau'' = \frac{1}{t^{3/2}}\frac{\partial^2 T}{\partial l^2}. \tag{6.6}$$

This allows for the transformation of the system (1.16), (1.17) to the following OIDEs:

$$0 = -\beta(2K'T + KT') + \alpha(K'' - KT^2 + K^3) + \alpha K'\int_0^l K^2\,\mathrm{d}l' + \tfrac{1}{2}(K + lK'), \tag{6.7}$$

$$\begin{aligned} 0 = {} & \beta\left(\frac{K'' - KT^2}{K} + \tfrac{1}{2}K^2\right)' + \alpha\left[\left(\frac{2K'T + KT'}{K}\right)' + 2TK^2\right] \\ & + \alpha T'\int_0^l K^2\,\mathrm{d}l' + \tfrac{1}{2}(T + lT'), \end{aligned} \tag{6.8}$$

where the prime now denotes differentiation with respect to l. System (6.7), (6.8) has a four-parametric class of solutions, which describe the vortex filaments conserving their shapes during time evolution, but with spatial scale growing as $\sqrt{t}$. Note, that the difference between the above system and equations (2.1), (2.2) is only in the last terms: $\frac{1}{2}(K + lK')$ and $\frac{1}{2}(T + lT')$ of (6.7), (6.8).

Finally, let us note that the system (1.16), (1.17) is invariant under the transformation $\beta \hookrightarrow -\beta, \alpha \hookrightarrow -\alpha, t \hookrightarrow -t$. This implies that the solutions of equations (6.7), (6.8) with negative α, β, correspond to the solutions with positive α, β, but with a decreasing spatial scale. Such solutions exist only up to some finite time.

7. Conclusions

In the paper, we analysed quasi-static solutions of quantum vortex motion. Existence of this class of solutions for the dissipative equation, (1.8), is not intuitive. We may

https://doi.org/10.1017/S0022112002003282 Published online by Cambridge University Press

expect that the shrinking vortex filament $\boldsymbol{s}(\xi, t)$, cannot be isometric to its initial condition $\boldsymbol{s}(\xi, 0)$ for arbitrary t. Nevertheless, it is possible, when the vortex has infinite length, which still remains infinite during its evolution. The Hasimoto soliton is a pulse-like solution of a non-dissipative system. Our solutions can be interpreted as kink-like solutions, which may exist for dissipative systems. In the simplest case, when the corresponding isometric transformation of $\boldsymbol{s}(\xi, 0)$ onto $\boldsymbol{s}(\xi, t)$ is a pure translation, we can interpret our analytic solution as a travelling wave which separates the region with vorticity from the region without vorticity. This interpretation would be more justified, if our vorticity field were defined not on a line, but on a plane or in a volume.

The interesting question (raised by one of the referees) is: how robust are the new solutions if the LIA is replaced by the exact Biot-Savart law. Since the filaments presented in figures 3 and 4 are tightly wrapped, we may expect that their dynamics are strongly influenced by the non-local terms, not captured by LIA, which is therefore not a satisfactory approximation. On the other hand, it is possible, that the mutual induction, calculated on a given roll, arising from its two neighbouring rolls, cancels out to some extent, which prevents the rolls from rotating around each other (see Ricca 1994 for the analysis of motion of helical vortex filaments under the Biot-Savart law). A different situation is the case, presented in figure 1, in which the vortex has two oppositely oriented parallel asymptotes. In such a case, we may expect that the non-local terms lead to, more or less, uniform additional motion in the direction perpendicular to the plane containing the two asymptotes. The another approach to the question, is to consider first the vortex dynamics governed by the Biot-Savart law, with an additional friction term resulting from the action of the normal helium component,

$$\dot{\boldsymbol{s}} = \boldsymbol{V}_i + \bar{\alpha}\boldsymbol{s}' \times \boldsymbol{V}_i, \tag{7.1}$$

where $\boldsymbol{V}_i$ is given by (1.1), and ask if (7.1) has the quasi-static solutions. The question seems to be both interesting and difficult. To our knowledge, the problem is still open, even in the case of conservative dynamics ($\bar{\alpha} = 0$). For example, it is not known if there exists a solution of Biot-Savart law corresponding to the Hasimoto soliton.

We expect that the method proposed in § 2, where the system of stationary equations for the curvature and the torsion was alternatively derived, can be generalized to the case when vorticity or velocity fields are defined in more dimensions. This may allow the analysis of quasi-static solutions for more general flows. For the static solution $\Phi_i(x, y, z, t) = \Phi_i(x, y, z, 0), t \in R$, where Φ_i are the vector or scalar fields of the problem. For quasi-static solutions, in general, $\Phi_i(x, y, z, t) \neq \Phi_i(x, y, z)$, but there exists an isometric transformation $\mathscr{T}(t)$, transforming the field configuration $\Phi_i(x, y, z, 0)$ into $\Phi_i(x, y, z, t)$. This implies that quasi-static solutions can be considered as generalizations of the static solution. In the particular case when $\mathscr{T}$ is pure translation, we may expect that our solutions will describe travelling waves, but when $\mathscr{T}$ is a superposition of translation and rotation, the corresponding solution will be more general.

The author would like to thank Bogdan Kazmierczak, Konrad Bajer and Renzo Ricca for helpful discussions and pointing out some items in the literature. This work was partially supported by the British/Polish Joint Research Collaboration Programme of the British Council and Komitet Badan Naukowych (KBN) and KBN grant 7T07A 01817. The author would like to thank the staff of the School of Mathematical Sciences of the University of Exeter for their hospitality.

https://doi.org/10.1017/S0022112002003282 Published online by Cambridge University Press

REFERENCES

Barenghi, C. F., Bauer, G. H., Donnelly, R. J. & Samuels, D. C. 1997 Superfluid vortex lines in a model of turbulent flow. *Phys. Fluids* **9**, 2631–2643.

Hasimoto, H. 1972 A soliton on a vortex filament. *J. Fluid Mech.* **51**, 477–485.

Idowu, O. C., Kivotides, D., Barenghi, C. F. & Samuels, D. C. 2000 Equation for self-consistent superfluid vortex line dynamics. *J. Low. Temp. Phys.* **120**, 269–280.

Langer, J. & Perline, R. 1991 Poisson geometry of the filament equation. *J. Nonlinear Sci.* **1**, 71–93.

Lipniacki, T. 2001*a* On quantum turbulence in superfluid ^{4}He. *Arch. Mech.* **53**, 23–43.

Lipniacki, T. 2001*b* Evolution of the line-length density and anisotropy of quantum tangle in ^{4}He. *Phys. Rev.* B **64**, 214516-1-9.

Lipniacki, T. 2002 Self similar solutions of quantum vortex motion. In *Advances in Turbulence IX, Proc. Ninth European Turbulence Conf.* (ed. I. P. Castro, P. E. Hancock & T. G. Thomas), pp. 665–668. CIMNE.

Nakayama, K., Segur, H. & Wadati, M. 1992 Integrability and the motion of curves. *Phys. Rev. Lett.* **69**, 2603–2606.

Nemirowskii, S. K. & Fiszdon, W. 1995 Chaotic quantized vortices and hydrodynamic processes in superfluid helium. *Rev. Mod. Phys.* **67**, 37–84.

Onuki, A. 1985 Line motion in terms of nonlinear Schrödinger equations. *Prog. Theor. Phys.* **74**, 979–996.

Ricca, R. L. 1991 Intrinsic equations for the kinematics of a classical vortex string in higher dimensions. *Phys. Rev.* A **43**, 4281–4288.

Ricca, R. L. 1992 Physical interpretation of certain invariants for vortex filament motion under LIA. *Phys. Fluids* A **4**, 938–944.

Ricca, R. L. 1994 The effect of torsion on the motion of a helical vortex filament. *J. Fluid Mech.* **273**, 241–259.

Ricca, R. L. 1996 The contributions of Da Rios and Levi–Civita to asymptotic potential theory and vortex filament dynamics. *Fluid Dyn. Res.* **18**, 245–268.

Ricca, R. L., Samuels, D. C. & Barenghi, C. F. 1999 Evolution of vortex knots. *J. Fluid. Mech.* **391**, 29–44.

Schwarz, K. W. 1985 Three-dimensional vortex dynamics in superfluid ^{4}He: line–line and line–boundary interactions. *Phys. Rev.* B **31**, 5782–5804.

Schwarz, K. W. 1988 Three-dimensional vortex dynamics in superfluid ^{4}He: homogeneous superfluid turbulence. *Phys. Rev.* B **38**, 2398–2417.

Schwarz, K. W. & Rosen, J. R. 1991 Transient behavior of superfluid turbulence in a large channel. *Phys. Rev.* B **44**, 7563–7577.

https://doi.org/10.1017/S0022112002003282 Published online by Cambridge University Press